BioResearch Open Access
Volume 2, Number 3, June 2013

DOI: 10.1089/biores.2013.0005

Near-Infrared Optical Imaging for Monitoring the Regeneration of Osteogenic Tissue-Engineered Constructs

Elizabeth A. Cowles,[1] Joy L. Kovar,[2] Evan T. Curtis,[1] Huihui Xu,[1] and Shadi F. Othman[1]

Abstract

Millions of cases of bone injury or loss due to trauma, osteoporosis, and cancer occur in the United States each year. Because bone is limited in its ability to regenerate, alternative therapy approaches are needed. Bone tissue engineering has the potential to correct musculoskeletal disorders through the development of cell-based substitutes for osteogenic tissue replacement. Multiple medical imaging techniques such as magnetic resonance microscopy (MRM) were investigated recently; these techniques are able to provide useful information on the anatomical and structural changes of developing bone. However, there is a need for noninvasive approaches to evaluate biochemical constituents and consequent compositional development associated with growing osteogenic constructs. In this study, near-infrared (NIR) optical imaging with a bone-specific NIR-targeted probe, IRDye® 800CW BoneTag™ (800CW BT), was applied in this study to longitudinally visualize regions of mineralization of tissue-engineered bone constructs *in vivo*. A fluorescent cell-based assay was performed to confirm the preferential binding of 800CW BT to the mineralized matrix of differentiated osteogenically driven human mesenchymal stem cells (*h*MSCs) *in vitro*. The *h*MSCs were seeded onto a biocompatible gelatin scaffold, allowed to develop, and implanted into a mouse model. Engineered constructs were examined *in vivo* using NIR imaging for bone mineralization, paired with MRM for verification of developing tissue. Results showed that NIR imaging with 800CW BT labeling can effectively assess the calcification of the developing osteogenic constructs, which is consistent with the analysis of excised tissue using NIR microscopy and histology. In conclusion, this study evaluated bone-like function of regenerating bone through tracking calcium deposition via NIR optical imaging with a fluorophore-labeled probe in a noninvasive manner.

Key words: magnetic resonance microscopy; near-infrared imaging; tissue engineering; tissue-engineered bone

Introduction

Millions of cases of bone injury or loss due to trauma, osteoporosis, and cancer occur in the United States each year.[1] Because bone is limited in its ability to regenerate and remodel, natural healing is often insufficient. Though allogeneic and autologous transplants are clinically performed, their use is limited due to the risk of the infectious and painful procedure.[2] Therefore, an alternative strategy, bone tissue engineering (TE)—which seeks to correct musculoskeletal disorders through the development of cell-based substitutes for osteogenic tissue replacement—is needed. TE involves the use of progenitor cells, biocompatible scaffolds, and duplication of differentiation and growth factors to allow for cell growth and differentiation.[3,4] For instance, mesenchymal stem cells (MSCs) can be stimulated to differentiate into osteoblasts, chrondrocytes, or adipocytes, and can be used as bone progenitor cells that, when seeded onto a three-dimensional scaffold with appropriate stimulant, can form osteocytic, chondrocytic, or adipocytic tissue.[5,6]

Imaging modalities has been used to understand the dynamic evolution of osteogenic engineered tissues both *in vitro* and *in vivo*, but each modality has limitations. For example, magnetic resonance microscopy (MRM) has been successfully applied to assess the development and regeneration of tissue-engineered bone;[7,8] however, relatively low proton density and short T_2 relaxation times associated with bone tissues often dampen signal intensities on the magnetic resonance images in late stages of osteogenesis. X-ray microcomputed tomography of bone exhibits high resolution and contrast, but the contrast is less apparent in the marrow and newly formed bone;[9] additionally the subjection of the tissue to ionizing radiation causes undesired damage and harm.[10] Finally, ultrasound is noninvasive but has a relatively low spatial resolution,

[1]Department of Biological Systems Engineering, University of Nebraska, Lincoln, Nebraska.
[2]LI-COR Biosciences, Lincoln, Nebraska.

making it difficult to visualize the compositional and structural changes in engineered bone constructs.[11] Near-infrared (NIR) optical imaging, on the other hand, with an appropriate fluorophore-labeled probe has been used successfully for noninvasive and longitudinal visualization of bone deposition *in vivo*.[12] In particular, IRDye® 800CW BoneTag™ (800CW BT), a calcium-chelating tetracycline-derivative conjugated to the NIR fluorophore IRDye 800CW, can bind to differentiated mineralized osteoblast cultures and effectively target *in vivo* native bone structures.[12]

In this article, we postulate that bone-like function of mesenchymally derived tissue-engineered bone constructs implanted in a mouse model can be monitored through tracking calcium deposition via NIR optical imaging with a fluorophore-labeled probe. To address this question, NIR optical imaging with 800CW BT labeling was used to monitor the process of osteogenesis through cell-based assays. The binding of the 800CW BT to mineral matrices of differentiated osteogenic-like cells was confirmed by von Kossa histological analysis. Once the preferential binding of 800CW BT for differentiated MSCs was identified, osteogenic tissue-engineered constructs were developed *in vitro* and implanted into a mouse model. Over time, 800CW BT was injected and visualized using NIR optical imaging *in vivo.* Finally, the osteogenic constructs were excised and subjected to additional histologic and NIR microscopy measurements to establish specificity of binding.

Materials and Methods

Cell-based assays and histology of monolayer

Human MSCs (*h*MSCs) isolated from adult human bone marrow were obtained commercially (PT-2501; Lonza, Basel, Switzerland). The cells were incubated in MSC basal medium (PT-3001 MSCGM™ Bullet Kit™; Lonza) during the expansion and growth process at 37°C and 5% CO_2. The *h*MSCs were isolated by removing unattached cells during media exchange; when *h*MSCs were ~80% confluent, cells were trypsinized and plated at a density of 3500 cells/mL in 24-well plates for a total cell number of 7000 cells as described previously.[13] One day after plating, the cells intended for osteogenic differentiation were stimulated using osteogenic induction medium (PT-3002 *h*MSC differentiation BulletKit™; Lonza) during the entire monolayer study, while the undifferentiated cells (unstimulated control group) were maintained in basal medium. The plates were evaluated at two different time points: the undifferentiated control group was evaluated at week 1, while the differentiated group was evaluated at week 4, necessary for comparable cell numbers between groups.

A fluorescent cell-based assay was used to evaluate binding efficiency of 800CW BT (LI-COR Biosciences, Lincoln, NE) as a marker for differentiation of osteogenic cells. The test was assessed in quadruplicate for the undifferentiated and differentiated cells. The probe was prepared by reconstituting 10 nmol of 800CW BT in 0.5 mL phosphate-buffered saline (PBS) immediately prior to use. Undifferentiated and differentiated cells were incubated for 1 h with 800CW BT in concentrations of 200, 100, and 50 nM, diluted in osteogenic media to measure the extent of mineralization. The cells were fixed with 10% formalin for 20 min and washed four times with 1× PBS + 0.05% Tween-20. The cells were blocked in Odyssey® Blocking Buffer (LI-COR) for 1.5 h and incubated for 1 h with TO-PRO-3® (Invitrogen Corporation, Carlsbad, CA) DNA stain (700 nm) diluted 1:5000. The cells were again washed four times with 1× PBS + 0.05% Tween-20. Fluorescence (excitation 774 nm, emission 805 nm) imaging data for the 800CW BT were collected using an Odyssey® CLx Infrared Imaging System (LI-COR). The relative fluorescent units (RFU) of undifferentiated and differentiated *h*MSCs were determined by applying a radiometric analysis of fluorescence (800-nm signal normalized to 700-nm signal). To inspect mineralization, the cells underwent von Kossa staining using 5% silver nitrate (S8157; Sigma-Aldrich, St. Louis, MO) after fixing in 10% formalin.[14] Assessment of the stains was conducted using a VWR VistaVision inverted microscope retrofitted with a Microsoft® LifeCam web camera for image acquisition.

Tissue-engineered construct preparation and implantation

Osteogenic tissue-engineered constructs were prepared using the *h*MSCs and a biodegradable sterile gelatin scaffold (Gelfoam®, Baxter Healthcare Corporation, Hayward, CA), trimmed into 3.5 mm × 3.5 mm × 4 mm sections and prewetted for 24 h in MSCGM™ (Lonza). The *h*MSCs were seeded onto the scaffold at a density of 10^6 cells/mL with the help of slight vacuum generated by a 20-mL syringe.[15] The scaffold-cell suspension was incubated at 37°C and 5% CO_2 for 2 h before transfer to basic media for 24 h.[16] Differentiation was induced the following day by culturing in osteogenic induction media. Following 4 weeks of *in vitro* culture, the constructs were implanted in male nude immunodeficient mice (nu/nuJ, Jackson Laboratories, Bar Harbor, ME). All animals and procedures used in this study were cared for and maintained under the supervision and guidelines of the University of Nebraska-Lincoln Institutional Animal Care and Use Committee. For the implantation surgery, the mice were anesthetized with 5% isoflurane. The area was sterilized with an iodine scrub and solution before implantation. The tissue-engineered construct was implanted in the subcutaneous region 2 cm distal to the scapula on the left side. An additional gelatin scaffold (cell-free construct) was presoaked for 24 h in basic media and implanted in the same location opposite the differentiated tissue construct on the right side to serve as control. A nonfluorescing silk suture (683G; Ethicon, Somerville, NJ) was used to close the incision. After 7 days, the suture was removed and the animals were monitored for 1 month using NIR optical and MRM imaging.

Imaging of TE constructs

The 800CW BT was prepared as stated previously to the concentration of 20 nmol/mL. All mice were anesthetized with 2% isoflurane during the imaging sessions. One week and 1 month after implantation, the mice were administered a 2 nmol (100 μL) intraperitoneal injection of 800CW BT, the recommended dose from previous studies.[12] Images (dorsal, left and right lateral views) were taken 24 h post-injection using the Pearl® Impulse Small Animal Imager (LI-COR). Each image was acquired at a resolution of 85 μm. Following NIR optical imaging, MRM studies were conducted *in vivo* using a 9.4-T (400 MHz for protons) 89-mm vertical bore scanner (Agilent Technologies, Santa Clara, CA) equipped with a

4-cm Millipede radiofrequency imaging probe and a 100 G/cm maximum triple axis gradients. MRM images were acquired using a fast spin-echo sequence with the following parameters: TR = 2000 ms, TE = 9 ms, field of view = 2.5 cm, 256 × 256 matrix, echo-train-length = 4 with 16 averages and 0.5-mm slice thickness.

Histology for osteoblast and calcium deposition

Following 1 month of *in vivo* regeneration, the mice were euthanized and tissue was harvested, a portion of which was sent to Histoserv Inc. (Germantown, MD) for hematoxylin and eosin (H&E) staining, to label nuclei of cells in the construct, and von Kossa staining, to identify area of mineralization. Histologic slides were examined by a board-certified pathologist for assessment of mineralization and calcium deposition. Additionally, a portion was frozen for sectioning (5 μm) and imaged with fluorescent microscopy.

Results

Monolayer: cell-based assay and histology

The fluorescent cell-based assay was performed in order to demonstrate the preferential binding of the 800CW BT to the mineral matrix of differentiated osteogenic *h*MSCs. Figure 1a shows the RFU of undifferentiated and differentiated *h*MSCs incubated in increasing 800CW BT concentrations (0–200 nM). The signal intensity for the differentiated osteogenic cells was 4.45 to 7.75 times higher than in the undifferentiated cells. To confirm mineralization, both groups were stained with silver nitrate for von Kossa evaluation, which showed black depositions when positive (Fig. 1b). Analysis of variance (ANOVA) confirmed a statistically significant difference between undifferentiated and differentiated cells at 200 nM 800CW BT ($p < 0.05$). ANOVA was performed using GraphPad Prism software (La Jolla, CA) to assess significance between treatment groups.

In vivo *implantation and* ex vivo *analysis*

The mice were imaged using NIR optical imaging at two time points. Figure 2 shows the white light (grayscale) and 800-nm fluorescent images (green) of a mouse at 1 week (Fig. 2a, b) and 1 month (Fig. 2c, d) post implantation. The control scaffold was apparent in the white light image at 1 week (Fig. 2a), while it could not be identified in the 1-month image (Fig. 2c). Additionally, the control scaffold did not show any fluorescence. The construct in the fluorescence image at 1 week contained a higher signal intensity compared with the surrounding tissue (Fig. 2b). The construct continued to regenerate for 1 month and exhibited a 4.5-fold increase in signal intensity and a 3.3-fold increase in area of regenerating tissue (Fig. 2d).

Figure 2e shows the results of MRM following NIR optical imaging at 1 month. MR signal intensity was reduced for the construct when compared with adjacent tissues. Figure 2f shows an area of black deposition on a von Kossa–prepared slide. The same slide was imaged using NIR microscopy at 800 nm, and Figure 2g shows fluorescence corresponding to the areas of mineralization. Figure 2h shows a portion of the excised tissue stained by H&E. From the histological analysis, the construct was determined to be highly calcified and appeared as bone.

Discussion

Previously, *in vitro* mineralization for bone-forming cells such as osteoblasts was quantified using a calcein bound to hydroxyapatite, a good biological marker for osteoblast activity, using a fluorescence multiwell plate reader at 530-nm emission.[17]

Native bone tissue formation and remodeling *in vivo* have been shown to be successfully assessed through the use of calcium-binding fluorescent dyes, which bind areas of mineralization and fluoresce in the NIR region of the spectrum.[12]

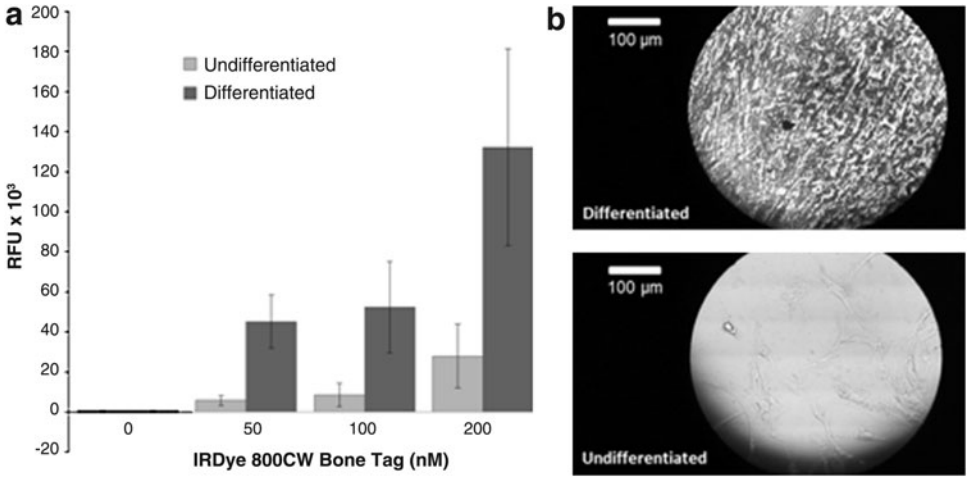

FIG. 1. Near-infrared (NIR) cell-based assay performed on the human mesenchymal stem cells (*h*MSC) monolayer to confirm the preferential binding of the IRDye 800CW BoneTag (800CW BT) to developed osteogenic cells. **(a)** Confluent cultures of undifferentiated and differentiated *h*MSCs were incubated in increasing 800CW BT concentrations (0–200 nM). Relative fluorescent units (RFU) data are plotted as means with standard deviations. Analysis of variance (ANOVA) showed a statistically significant difference between undifferentiated and differentiated cells at the 200 nM concentration ($p < 0.05$). **(b)** von Kossa staining of *h*MSC monolayer, microscopically imaged at 250× magnification.

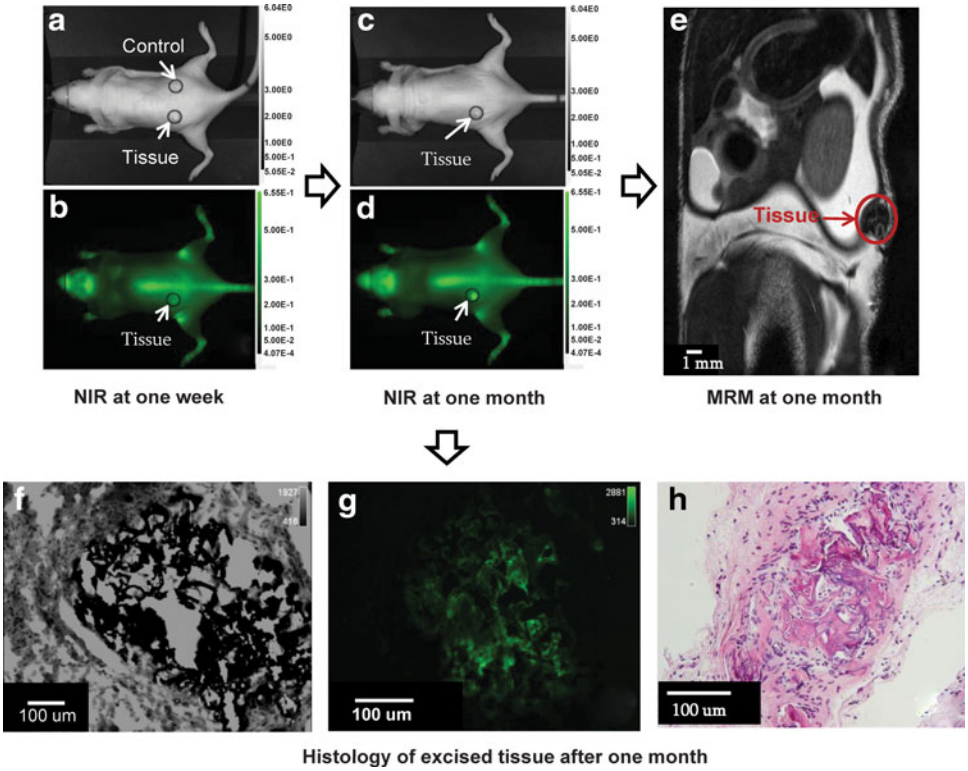

FIG. 2. Optical imaging of implanted osteogenic constructs (circled in red) in a mouse with corresponding histologic analysis confirming mineralization. The mice were injected 1 week **(a, b)** and 1 month **(c, d)** post-implantation with 800CW BT and evaluated 24 h later with NIR optical imaging. White light images **(a, c)** indicate location of differentiated and control implantation sites. NIR images taken at the same time points **(b, d)** indicate binding and labeling of osteogenic tissue constructs with 800CW BT reflected in higher signal intensities for these regions compared to the surrounding tissue. Following optical imaging, magnetic resonance microscopy (MRM) of the osteogenic constructs confirmed the presence of the tissue **(e)**. Following *in vivo* imaging, the osteogenic construct was excised and cut in 5-μm sections for microscopy of adjacent von Kossa **(f)** and NIR microscopy **(g)**. Additional histological analysis included hematoxylin and eosin staining of slides at 40× magnification **(h)**.

They have been shown to effectively label native skeletal features and bone mineralization remodeling processes, as well as preferentially bind mineral matrices of osteogenic differentiated MC3T3-E1 cells in culture. *In vivo* imaging in the NIR spectrum (650–900 nm) provides high sensitivity and signal-to-noise ratios compared with imaging at the visible wavelengths due to the reduced light absorption and scattering of NIR waves in biological tissues.[18]

Based on these findings, the use of 800CW BT was examined for effectively binding and labeling mesenchymally derived osteogenic constructs. In the cell-based assay, the results demonstrated the preferential binding of 800CW BT to the mineral matrix produced after differentiation. The signal intensity levels of the assay increased with increasing 800CW BT concentrations, indicating the cells did not reach a saturation level in the range of 0–200 nM; therefore, an optimal dose cannot be stated and should be investigated in future studies. Similar findings were observed previously with increasing concentrations of hydroxyapatite when studying calcein binding in osteoblast cells.[17] GLP toxicity data on IRDye 800CW and GMP quality dye are available, and a drug master file is on record with both U.S. and European regulatory agencies, which facilitates clinical translation.[19]

The 800CW BT successfully bound regions of mineralization in osteogenic construct but did not bind to the control scaffold. In addition, the control scaffold exhibited no autofluorescence at 800 nm. Since the construct was labeled at two time points, with greater signal intensity and signal area at the 1-month post-implantation compared with the 1-week time point, the results indicated a potential for periodically monitoring regenerating tissue-engineered osteogenic construct mineralization and remodeling processes. The 800CW BT persists in bone for an extended time period but progressively clears in a few weeks. A longitudinal study with a longer duration, as well as the use of a larger statistical sample size would assist in further promoting the benefit of this novel technology. MRM was used to indicate the location and size of the construct in relation to the NIR image prior to excising the tissue and performing histological analysis; the decreased signal intensity of the construct in the MR image indicated a relatively low number of hydrogen atoms and short T_2 relaxation time, which are typical traits of bone tissue as described previously.[20,21] After *in vivo* imaging, the construct was excised and underwent NIR microscopy to visualize binding of the 800CW BT to bone mineralization established with H&E and von Kossa

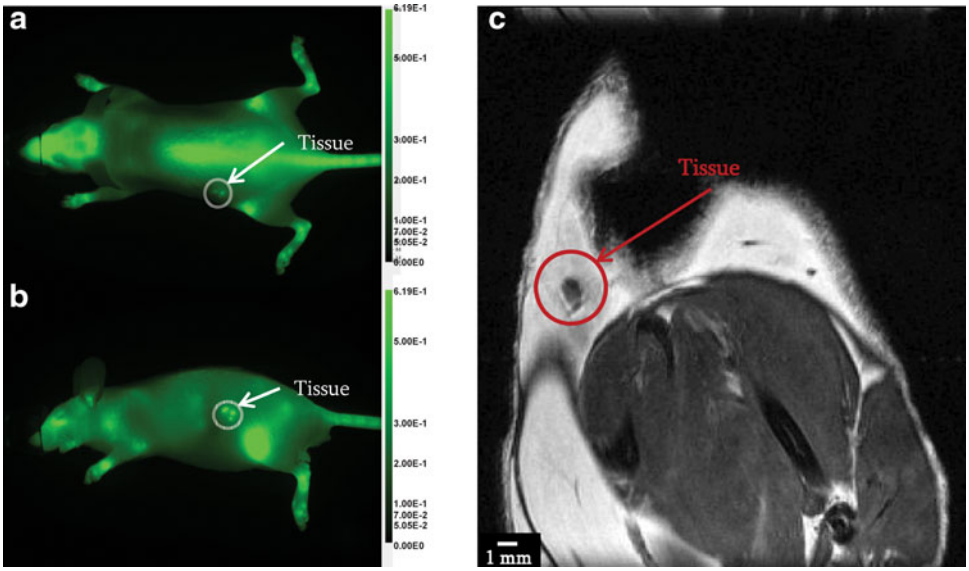

FIG. 3. NIR and MRM imaging of tissue-engineered construct highlighting penetration depth limitation in optical imaging as shown in the dorsal view **(a)**. By changing the mouse position, it was possible to avoid the penetration depth limitation as shown in the left view of the mouse **(b)**. MRM does not suffer from penetration depth limitation but susceptibility artifacts are present in the acquired coronal view **(c)**.

staining. However, von Kossa staining alone was reported to be insufficient to confirm that mineralization *in vitro* represents bone formation,[22] and our mineralization results were confirmed with H&E and von Kossa staining by a certified pathologist as well as NIR microscopy. With the successful preliminary results we have shown in this study, it would be prudent to include further matrix component characteristics in future work.

Although successful in longitudinal and noninvasive studies following osteogenesis, NIR optical imaging does exhibit limitations as an imaging modality. NIR is a planar imaging technology and proper orientation is needed or images will suffer from low penetration depth, especially as compared to modalities such as volumetric MRM. Figure 3 shows NIR images of the dorsal and left planes of an implanted construct. The dorsal view cannot fully visualize the entire construct due to low penetration depth (Fig. 3a), while the left view provides a complete image representation of the construct (Fig. 3b). Subcutaneous implants are easily visualized by NIR planar imaging though NIR tomography would give a more three-dimensional rendering similar to MRM.[23] MRM does not suffer from penetration depth limitation but lacks NIR specificity (Fig. 3c). In this specific subject, the construct was fragmented, unintentionally, into three pieces during surgery, which highlights the better specificity of optical imaging (identified the three pieces in the left view) compared with low signal intensity MRM image smeared with susceptibility artifact. Multimodal imaging has the potential to overcome the problems of individual imaging modalities by providing more comprehensive images of engineered construct evolution to fully examine the composition, structure, and function noninvasively.

Future applications of NIR probes in labeling of tissue-engineered osteogenic constructs should include examining the effect of advanced scaffolding technique such as bioprinted scaffolds.[24] In addition, NIR imaging may be used to monitor the produced mineral matrix under various factors, for example, vascular endothelial growth factor, which promotes vascularization,[25] or implantation of an osteogenic construct in a native bone location.[26] Additionally, future use of various NIR probes that fluoresce at different wavelengths could potentially allow for imaging of incremental increases in mineralization, which would lead to a better understanding of bone growth and remodeling mechanisms.[12] The nature of the high signal intensity obtained from 800CW BT to the desired target molecules provides a distinct advantage over the low-level signal of MRM in bone or the harmful ionizing radiation of X-ray and computed tomography. In conclusion, the presence of bone-like mineral deposition was evaluated noninvasively in osteogenic tissue-engineered constructs through tracking calcium deposition via NIR with a fluorophore-labeled probe.

Acknowledgments

The authors thank Mr. Vahid Khalilzad-Sharghi (Department of Biological Systems Engineering, University of Nebraska–Lincoln) for his assistance with MRM images. The authors also thank D. Michael Olive, PhD (SVS Consulting, Lincoln, NE), for a perceptive NIR discussion.

References

1. Laurencin CT, Ambrosio AM, Borden MD, et al. Tissue engineering: orthopedic applications. Annu Rev Biomed Eng. 1999;1:19–46.
2. O'Keefe RJ, Mao J. Bone tissue engineering and regeneration: from discovery to the clinic—an overview. Tissue Eng Part B Rev. 2011;17:389–392.
3. Griffith LG, Naughton G. Tissue engineering—current challenges and expanding opportunities. Science. 2002;295:1009–1014.
4. Sharma B, Elisseeff JH. Engineering structurally organized cartilage and bone tissues. Ann Biomed Eng. 2004;32:148–159.
5. Salgado AJ, Coutinho OP, Reis RL. Bone tissue engineering: state of the art and future trends. Macromol Biosci. 2004;4:743–765.
6. Service RF. Tissue engineers build new bone. Science. 2000;289:1498–1500.
7. Xu H, Othman SF, Hong L, et al. Magnetic resonance microscopy for monitoring osteogenesis in tissue-engineered construct in vitro. Phys Med Biol. 2006;51:719–732.

8. Potter K, Sweet DE, Anderson P, et al. Non-destructive studies of tissue-engineered phalanges by magnetic resonance microscopy and X-ray microtomography. Bone. 2006;38: 350–358.
9. Jones JR, Atwood RC, Poologasundarampillai G, et al. Quantifying the 3D macrostructure of tissue scaffolds. J Mater Sci Mater Med. 2009;20:463–471.
10. Wolbarst AB. *Physics of Radiology, 2nd ed.* Medical Physics Publishing: Madison, WI, 2005.
11. Kim K, Jeong CG, Hollister SJ. Non-invasive monitoring of tissue scaffold degradation using ultrasound elasticity imaging. Acta Biomater. 2008;4:783–790.
12. Kovar JL, Xu X, Draney D, et al. Near-infrared-labeled tetracycline derivative is an effective marker of bone deposition in mice. Anal Biochem. 2011;416:167–173.
13. McBeath R, Pirone DM, Nelson CM, et al. Cell shape, cytoskeletal tension, and RhoA regulate stem cell lineage commitment. Develop Cell. 2004;6:483–495.
14. Maniatopoulos C, Sodek J, Melcher AH. Bone formation in vitro by stromal cells obtained from bone marrow of young adult rats. Cell Tissue Res. 1988;254:317–330.
15. Dennis JE, Haynesworth SE, Young RG, et al. Osteogenesis in marrow-derived mesenchymal cell porous ceramic composites transplanted subcutaneously: effect of fibronectin and laminin on cell retention and rate of osteogenic expression. Cell Transplant. 1992;1:23–32.
16. Gao JZ, Dennis JE, Solchaga LA, et al. Tissue-engineered fabrication of an osteochondral composite graft using rat bone marrow-derived mesenchymal stem cells. Tissue Eng. 2001; 7:363–371.
17. Hale LV, Ma YF, Santerre RF. Semi-quantitative fluorescence analysis of calcein binding as a measurement of in vitro mineralization. Calcif Tissue Int. 2000;67:80–84.
18. Kovar JL, Simpson MA, Schutz-Geschwender A, et al. A systematic approach to the development of fluorescent contrast agents for optical imaging of mouse cancer models. Anal Biochem. 2007;367:1–12.
19. Marshall MV, Draney D, Sevick-Muraca EM, et al. Single-dose intravenous toxicity study of IRDye 800CW in Sprague-Dawley rats. Mol Imaging Biol. 2010;12:583–594.
20. Xu H, Othman SF, Magin RL. Monitoring tissue engineering using magnetic resonance imaging. J Biosci Bioeng. 2008; 106:515–527.
21. Othman SF, Curtis ET, Plautz SA, et al. MR elastography monitoring of tissue-engineered constructs. NMR Biomed. 2012;25:452–463.
22. Bonewald LF, Harris SE, Rosser J, et al. von Kossa staining alone is not sufficient to confirm that mineralization in vitro represents bone formation. Calcif Tissue Int. 2003;72: 537–547.
23. Zilberman Y, Kallai I, Gafni Y, et al. Fluorescence molecular tomography enables in vivo visualization and quantification of nonunion fracture repair induced by genetically engineered mesenchymal stem cells. J Orthop Res. 2008;26:522–530.
24. Fielding GA, Bandyopadhyay A, Bose S. Effects of silica and zinc oxide doping on mechanical and biological properties of 3D printed tricalcium phosphate tissue engineering scaffolds. Dent Mater. 2012;28:113–122.
25. Wernike E, Montjovent MO, Liu Y, et al. VEGF incorporated into calcium phosphate ceramics promotes vascularisation and bone formation in vivo. Eur Cell Mater. 2010;19:30–40.
26. Uusitalo H, Rantakokko J, Ahonen M, et al. A metaphyseal defect model of the femur for studies of murine bone healing. Bone. 2001;28:423–429.

Address correspondence to:
Shadi F. Othman, PhD
Department of Biological Systems Engineering
University of Nebraska at Lincoln
249 L.W. Chase Hall
Lincoln, NE 68583

E-mail: sothman2@unl.edu